Metabolic Engineering 12 (2010) 123–128

Contents lists available at ScienceDirect

Metabolic Engineering

journal homepage: www.elsevier.com/locate/ymben

Regular Article

Improved computational performance of MFA using elementary metabolite units and flux coupling

Patrick F. Suthers, Young J. Chang, Costas D. Maranas *

Department of Chemical Engineering, The Pennsylvania State University, University Park, PA 16802, USA

ARTICLE INFO

Article history:
Received 23 March 2009
Received in revised form
14 September 2009
Accepted 7 October 2009
Available online 27 October 2009

Keywords:
Metabolic flux analysis
Isotope labeling
Optimization
Constraint-based modeling
Experimental design

ABSTRACT

Extending the scope of isotope mapping models becomes increasingly important in order to analyze strains and drive improved product yields as more complex pathways are engineered into strains and as secondary metabolites are used as starting points for new products. Here we present how the elementary metabolite unit (EMU) framework and flux coupling significantly decrease the computational burden of metabolic flux analysis (MFA) when applied to large-scale metabolic models. We applied these techniques to a previously published isotope mapping model of *Escherichia coli* accounting for 238 reactions. We find that the combined use of EMU and flux coupling analysis leads to a ten-fold decrease in the number of variables in comparison to the original isotope distribution vector (IDV) version of the model. In addition, using OptMeas the task of identifying additional measurement choices to fully specify the flows in the metabolic network required only 2% of the computation time of the one using IDVs. The observed computational savings reveal the rapid progress in performing MFA with increasingly larger isotope models with the ultimate goal of handling genome-scale models of metabolism.

1. Introduction

Carbon labeling has been used to elucidate metabolic pathways and biotransformations and, more recently, ^{13}C-metabolic flux analysis has allowed the determination of fluxes in metabolic models. Most of the models employed have been of fairly limited scope because of the computational challenges involved with flux elucidation, and the time-consuming nature of constructing the atom mappings. In particular, most of the models have included only pathways within or close to central metabolism (i.e., 25–50 reactions) (Kim et al., 2008). Exceptions include a recently published medium-sized model that contains 75 reactions (Antoniewicz et al., 2007b) and a large-scale model containing 238 reactions (Suthers et al., 2007). As more complex pathways are engineered into strains and as secondary metabolites are used as starting points for new products (e.g., pharmaceuticals), increasing the scope of models becomes important in order to analyze strains and drive improved product yields.

There have been a number of modeling contributions that have led to the expansion of the scope of metabolic flux analysis (MFA), in part by formalizing how to construct the resulting equations. One of the first such modeling contributions was the introduction of atom mapping matrices (AMM) (Zupke and Stephanopoulos, 1994) that track the transfer of carbon atoms from reactants to products. This concept was subsequently generalized in the form of isotopomer mapping matrices (IMM) (Schmidt et al., 1997). The use of IMMs enables the formulation of all isotopomer mass balances of a metabolite pool using isotopomer distribution vectors (IDV) to quantify the fraction of each metabolite present in a particular isotope form. The cumomer concept (Wiechert et al., 1999) was later introduced to first prove that there exists a unique IDV assignment that satisfies any given feasible flux distribution and subsequently devise an IDV identification procedure by solving a cascade of equations.

One of the recent model framework contributions is the elementary metabolite unit (EMU) framework (Antoniewicz et al., 2007a). This framework analyzes the atom transitions and retains only the relevant combinations that give rise to the experimentally measured mass distributions. Through its application, a significant reduction in the number of variables can be achieved, which leads to a reduction in the computations required for flux elucidation, confidence intervals (Antoniewicz et al., 2006; Kleijn et al., 2005) and degree of resolution (Suthers et al., 2007) of each flux. The EMU framework has previously been applied to medium-size network model of 75 reactions and 64 species (Antoniewicz et al., 2007b).

Using flux balance analysis under steady-state conditions we find that not all fluxes in a metabolic network are independent. One method for determining the relationship for fluxes is flux coupling analysis (Burgard et al., 2004). This method allows the straightforward and computationally efficient means of determining which fluxes are fully, partially, or directionally coupled. This

* Corresponding author. Fax: +1 814 865 7846.
E-mail address: costas@psu.edu (C.D. Maranas).

1096-7176/$ - see front matter © 2009 Elsevier Inc. All rights reserved.
doi:10.1016/j.ymben.2009.10.002

result suggests that the confidence interval needs to be calculated only once per group of fully coupled fluxes, thus allowing for a reduction in the computations required for statistical analysis.

As the scope of isotope mapping models increases, the number of mass isotope distribution measurements needed to fully elucidate fluxes grows accordingly. The OptMeas method was recently proposed to determine measurement sets that enable flux elucidation using incidence structure analysis (Chang et al., 2008). The original implementation relied on an IDV description to track isotope labeling. The method was successfully used to suggest additional measurements for flux elucidation in a large-scale isotope mapping model. Although the method was scalable to large-scale models, improved efficiency would likely be needed for its application to models of significantly increased scope, such as genome-scale models.

In this report, we describe the application of the EMU framework and flux coupling to the large-scale isotope mapping model of *Escherichia coli* that includes the pathway for producing amorphadiene, a precursor to the antimalarial drug artemisinin. Their combined use led to substantial reductions in problem sizes and computational times for both flux elucidation and identification of additional measurements.

2. Materials and methods

For all calculations, the simulated environment was aerobic glucose minimal medium, and follows the values used in Suthers et al. (2007). Except where noted otherwise, all mass isotopomer distribution measurements, the isotope mapping model and atom transitions were identical to those in Suthers et al. (2007). Briefly, the model includes all reactions of Embden–Meyerhoff–Parnas (EMP) and Entner–Doudoroff (ED) glycolysis, the tricarboxcylic acid (TCA) cycle, and the pentose phosphate pathway (PPP). In addition, anaplerotic reactions and amino acid biosynthesis and degradation pathways are accounted for. The model enforces the explicit balancing of all metabolic cofactors (e.g., ATP, NADH, NADPH) and included reactions for energy generation via substrate-level and oxidative phosphorylation as well as transhydrogenase activity. Finally, the reactions enabling the production of amorphadiene in *E. coli* are also included in the model.

The EMU framework was implemented in Python by following the algorithm outlined in (Antoniewicz et al., 2007a). Briefly, the code first parses the network and atom transitions. A list of source metabolites and measurements are read and the measurements are traced back to the corresponding EMUs. This procedure continues until a source metabolite is reached and all EMUs are traced. The implementation accounts for symmetric metabolites and can also determine the reduced EMU network for isotopic steady-state conditions. Flux elucidation calculations and degree of resolution calculations were performed using CONOPT 3 accessed within the GAMS modeling environment as described in Suthers et al. (2007), except for replacing isotope balances with EMU balances. The block decomposition method (Young et al., 2007) was used to group the EMU balances. The flux coupling was performed as previously described (Burgard et al., 2004). Calculations were performed using CPLEX 11 accessed within the GAMS modeling environment. The resulting coupling output was parsed to extract those reactions that were fully coupled, as was the constant ratio needed to interconvert their flux values. The EMU network generation code is available at the authors' website (http://maranas.che.psu.edu).

The OptMeas framework uses incidence structure analysis to determine the relaxed identifiability condition (Chang et al., 2008). Briefly, this analysis abstracts the original algebraic system of equations by assigning variables to equations based on their incidence information. Each variable can be assigned to at most one equation, and conversely each equation can have as an output up to one variable. All unassigned variables are denoted as free variables and they must be measured to fully determine the system. In the original implementation, the variables were fluxes and IDVs. In the current work, EMUs replaced the IDVs, and the full EMU network was used during the construction of the incidence matrix. All input files were generated using Python code. The solution procedure follows that in Chang et al. (2008) using CPLEX 11 Concert technology and the measurement costs were set so that they corresponded to that of the previous work. The complete details of the EMU OptMeas extension are found in Appendix A.

3. Results and discussion

3.1. Flux elucidation

Application of the EMU framework to the large-scale isotope mapping model of an amorphadiene producing strain of *E. coli* (Suthers et al., 2007) resulted in a large reduction in the number of variables, as shown in Table 1. Whereas the full isotopomer model contains 17,346 isotopomers, there are only 1215 EMU species (available as supplementary material). Such comparisons of the two modeling frameworks have been reported for other systems (Antoniewicz et al., 2007a; Young et al., 2007). However, the number of actual mass isotopomers in the EMU network (i.e., 3912) is a more relevant comparison, as these are the variables fed to the solver. As seen in Table 1, there is still a substantial reduction in this number, with the EMU network containing only 22.6% of the total number of variables that the original isotopomer model did. The savings are even more substantial for the reduced EMU model, which takes advantage of isotopic steady-state to eliminate redundant variables. Here, the reduced EMU network is only 14.1% of the size of the IMM version.

The reduction in variables was only slightly better for the reduced isotope mapping model, which removed pathways that yielded identical labeling given the labeled substrate used in the experiment. Here, there were 20.8% and 11.0% of the variables in the complete and reduced EMU networks. As expected, solving the EMU representation for flux elucidation with the experimental measurements from Suthers et al. (2007) yielded comparable results to and was also substantially faster than the isotopomer representation. In all cases, the predicted mass isotopomer labeling patterns are identical when using either isotopomers or EMUs in the calculations given flux values, in agreement with Antoniewicz et al. (2007a). Because flux elucidation is a large nonlinear optimization problem, we performed multiple solutions of the problem from different initial conditions as described previously (Suthers et al., 2007). We note that there were relatively fewer instances of solutions above the χ^2 cutoff determined in the previous study. This result could arise from the fact that there are fewer tri-linear and higher terms in the EMU representation and thus the solver was more effective in finding better local optima. The best solutions had the same objective values in both representations.

The results from flux coupling analysis for the reduced isotope mapping model are summarized in Fig. 1. Here we can see that 78 of the 270 fluxes in this isotope model were involved in 14 fully coupled groups. Most of the groups are pairs of reactions, e.g., MALS and ICL. The largest group is that connected to the biomass equation, consistent with the results seen for other metabolic networks (Burgard et al., 2004). Also notable is that the amorphadiene production pathway forms a fully coupled module of nine fluxes (top right). In Suthers et al. (2007) both the growth rate and the amorphadiene production rate were fixed to

Table 1
Comparison of isotopomer and EMU representations of the large-scale isotope mapping model of *E. coli*.

Isotopomer model			EMU model		EMU reduced model	
# of carbons (size)	Metabolites	Isotopomers	EMU species[b]	Mass isotopomers	EMU species	Mass isotopomers
Full model[a]						
0	53	0				
1	11	22	495	990	305	610
2	11	44	313	939	203	609
3	22	176	209	836	135	540
4	23	368	101	505	66	330
5	25	800	67	402	37	222
6	31	1984	18	126	10	70
7	23	2944				
8	1	256	6	54	3	27
9	11	5632	6	60	3	30
10	5	5120				
Total	216	17346	1215	3912	762	2438
Reduced model						
0	48	0				
1	8	16	378	756	202	404
2	8	32	240	720	132	396
3	14	112	147	588	78	312
4	18	288	68	340	40	200
5	18	576	50	300	22	132
6	21	1344	16	112	8	56
7	21	2688				
8	1	256	5	45	2	18
9	7	3584	5	50	2	20
10	5	5120				
Total	169	14016	909	2911	486	1538

[a] Full and reduced models refer to the complete and the isotope model which has removed redunant labeling pathways, as described in Suthers et al. (2007).
[b] EMU species were also refered to as EMU variables in Antoniewicz et al. (2007a).

experimentally observed values. The flux coupling analysis results thus explain why as many as 100 fluxes were fixed due to stoichiometry alone. Using the flux coupling results also eliminates confidence interval calculations for 14% of the non-fixed reactions, since they need to be performed just once per group. These savings are afforded when using either the isotopomer or EMU representations during the flux elucidation calculations.

The incorporation of flux coupling constraints into the flux elucidation problem offered a moderate improvement in computation speed for both the isotopomer (4%) and EMU (3%) representations and is likely solver dependent. As before, the dominant factor in the time of an individual calculation was the use of the EMU representation, and flux coupling contributed mostly to a reduction in the number of flux elucidation optimizations required. Using both EMU and flux coupling for these flux range calculations yielded identical flux ranges as those in Suthers et al. (2007) but at reduced computational burden.

3.2. Measurement sets

The structure of the incidence matrix for OptMeas when using EMUs is shown in Fig. 2. The organization is similar to that of Fig. 2 in Chang et al. (2008), with the isotopic distributions replaced by EMU mass distributions. The balances around the metabolites have been partitioned into production and consumption terms. We introduced aggregate effluxes to partition the balance equations in order to minimize the possible linear dependency in the square system resulting from the incidence structure analysis (see Appendix A). As noted in Antoniewicz et al. (2007a), EMU balances occur in two forms: linear equations when all atoms in a product EMU come from a single reactant metabolite and nonlinear convolutions when there is more than one reactant contributing to the labeling of the product EMU. The equations for these terms are likewise segregated in the incidence matrix. For each EMU species, the sum of the mass isotopomers vector (MDV) variables sum to one and thus the MDVs are linearly dependent. Because of this fact, as with the IDV version of OptMeas, we excluded one of the mass isotopomers from each EMU species (i.e., the fully labeled one).

We applied OptMeas to the large-scale *E. coli* model (Suthers et al., 2007) using relative measurement costs equivalent to those in Chang et al. (2008) with the addition of metabolites from central metabolism that have been used before as measurements candidates in MFA such as pep, akg, cit, and succ. All abbreviations are from Suthers et al. (2007). The EMU version of OptMeas suggested flux measurements and mass distribution vector (MDV) measurements as indicated in Table 2. Except for the addition of citrate, these results are directly comparable to those obtained previously. We verified that measuring the full length MDV of citrate was indeed an effective addition to the measurement set and resulted in a smaller (better) objective value during the TestUniq procedure (Chang et al., 2008) that evaluates the uniqueness of the solution given the measurement set. This measurement was effective in the determination of fluxes because some fluxes in the TCA were individually inherently unidentifiable using stationary MFA (Chang et al., 2008). Measuring citrate thus aided in the determination of metabolite labeling patterns and flux ratios.

We note that there could be some bias in measurement selection since the EMU network is itself constructed from the list of all measurement options (and their intermediates). As noted above, we sought to reduce this bias by increasing the available measurements to compounds well beyond those in Suthers et al. (2007). We also found that increasing the network to include all full length mass isotopomer distributions did not impact the suggested measurements. Ultimately, MFA hinges on experimental

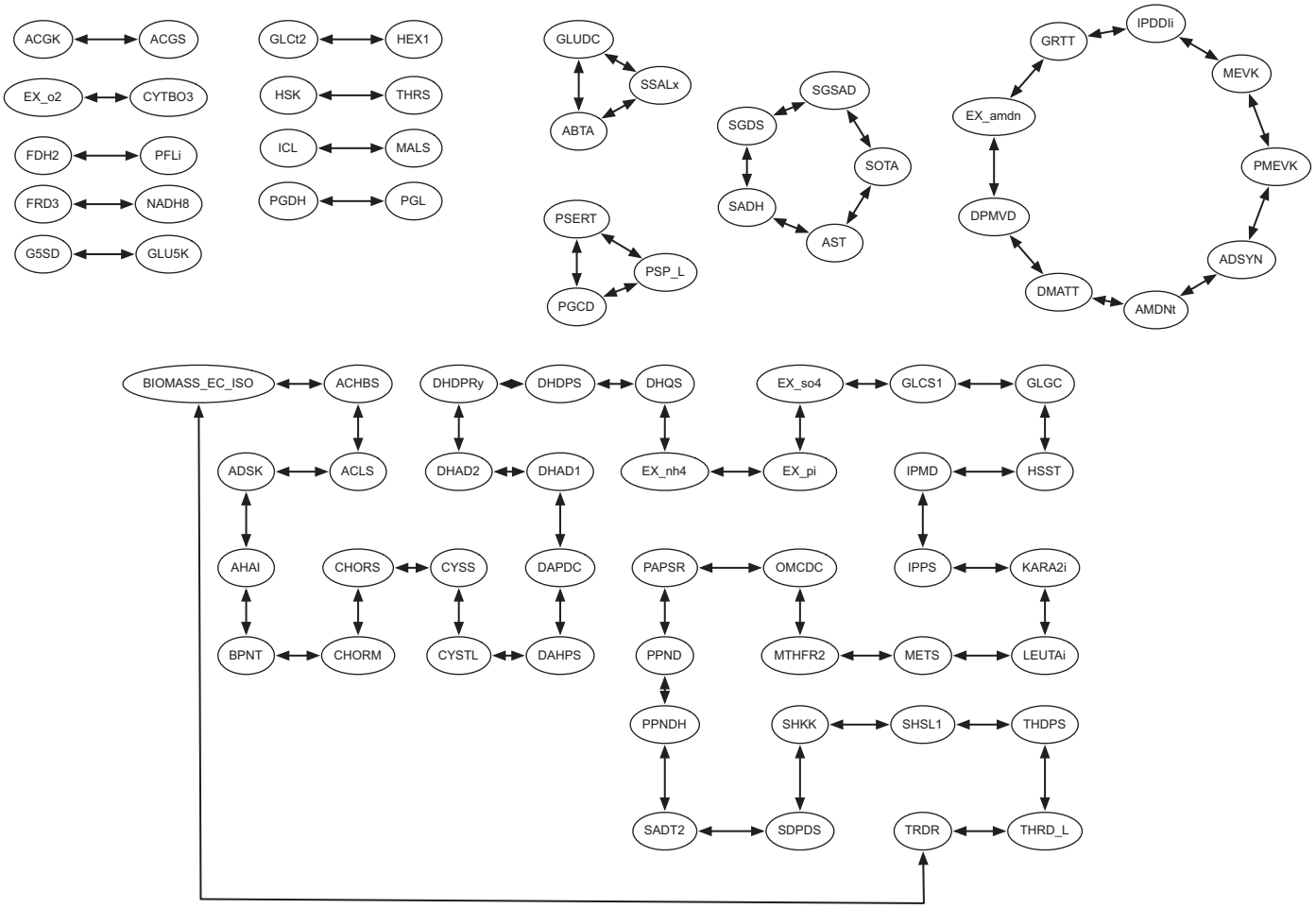

Fig. 1. Fully coupled fluxes in the large-scale isotope mapping model. Reactions names (ovals) are grouped into fully coupled groups connected by lines. The flux of each reaction in a group can be determined by multiplying a constant scalar to that of another member. Reaction abbreviations follow those in the *E. coli* model *i*JR904 (Reed et al., 2003).

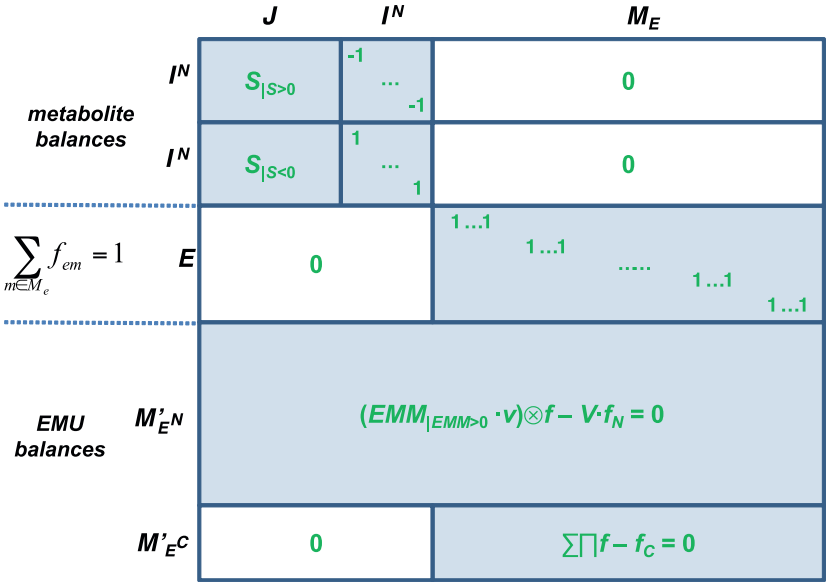

Fig. 2. Incidence matrix of MFA for OptMeas with EMU representation. Here *M*' is the same as *M* except that all linearly dependent mass isotopomers are excluded for each EMU. The shaded submatrices correspond to structurally nonzero regions.

Table 2
OptMeas suggested measurement sets.

Required fluxes	Growth rate (BIOMASS_EC_ISO) Amorphadiene production (AMDNt) Acetate production (ACt6) Glucose uptake rate (EX_glc-d) Oxygen uptake rate (EX_o2) Non-growth associated ATP maintenance (ATPM)
Required mass distribution vector (MDV) measurements	Amino acids: ala, arg, asp, glu, ile, leu, lys, met, phe, pro, ser, thr, val; organic acid citrate
Interchangeable mass distribution vector (MDV) measurements	1) akg plus two from {gly, tyr, ac} or 2) {gly, tyr, ac co2}

measurements and their availability. Thus a listing of available measurements is likely to be known and the EMU network can be constructed by using all of them during the generation process. If all the provided measurements are insufficient, then unresolved fluxes will be identified during the OptFlux procedure.

A number of significant advantages to using the EMU-based implementation of OptMeas are observed as opposed to the IMM-based one. Specifically, here we did not pre-select any of the measurements in the set, instead allowing OptMeas to choose all of them in a single step. Moreover, the calculation time was only about 2% that of the IDV implementation for which all of the amino acid measurements used in Suthers et al. (2007) were chosen *a priori*. The decrease in computation time is not only due to a significantly reduced matrix size (which is dominated by the number of IDV or EMU mass isotopomers), but also because the number of rows with three or more variables is decreased. These substantial improvements suggest that the EMU-based implementation is a more scalable choice for genome-scale model sizes. Additionally, this rapid computation time would enable the exploration of an increased number of alternative measurement costs, as well as the identification and elimination of suboptimal solutions.

We also incorporated flux coupling results to the TestUniq formulation during testing of the measurement sets proposed by OptMeas. It is used to allow only one representative for each coupled set into the objective, which reduces counting fluxes that do not have unique solutions multiple times. For the same measurement set, TestUniq gave the same results for both the isotopomer and EMU representations, however the EMU calculations were faster. When flux coupling was omitted from TestUniq and all fluxes appeared in the objective, the problem took a longer duration to solve, but again the objective value for both the isotopomer and EMU representations were the same.

4. Summary

We have described how the EMU framework and flux coupling can significantly decrease the computational burden that arises as the scope of isotope mapping models increase. These occur in both the speed (using EMU) and number (using flux coupling) of solutions necessary for flux elucidation and the calculation of confidence intervals. By being readily scalable, the EMU representation enables larger models to be constructed and computationally evaluated. Alternatively, the computational savings can be used to generate more searches for the best local optimum.

The computation efficiency afforded by the use of EMUs carried over into the OptMeas approach when determining minimal measurement sets for the large-scale isotope mapping model. Not only were we able to calculate these in approximately 2% of the time of that for the IDV version, but we could begin with no measurements given *a priori*, as OptMeas could do for smaller models as described in Chang et al. (2008).

Acknowledgment

This work was supported by DOE grant DE-FG02-05ER25684.

Appendix A

Mathematical model of MFA using EMU variables

We define the following sets and variables to model the EMU networks:

Sets

$I=\{i\}$:	metabolite pools
$I^N \subset I$:	intermediary metabolites
$J=\{j\}$:	fluxes
$E=\{e\}$:	elementary metabolite units (EMUs)
$E^c \subset E$:	combined EMUs
$E_i \subset E \mid E^C$:	EMUs from metabolite $i \in I$
$E^N = \bigcup_{i \in I^N} E_i$:	EMUs corresponding to intermediary metabolites
$E_e \subset E$:	EMUs that produce combined EMU $e \in E^C$
$M_e=\{m\}=\{0, 1, \ldots, n_e\}$:	mass isotopomers of EMU $e \in E$ that has n_e carbons

Variables:

$v_j \geq 0$ $j \in J$:	flux values
$f_{em} \in [0,1]$ $m \in M_e$, $e \in E$:	mass isotopomer fractions

We define EMU mapping matrix $EMM^j_{e' \to e}$ that accounts for the stoichiometry of flux j from EMU e' to e. $EMM^j_{e' \to e} > 0$ if e' produces e through j (mostly integral but could be fractional when e is an EMU of a symmetric molecule). Then we can write steady-state balance equations as

$$\sum_j S_{ij} v_j = 0 \quad i \in I^N \tag{1'}$$

$$\sum_{m \in M_e} f_{em} = 1 \quad e \in E \tag{2}$$

$$\sum_{e' \in E} \left(\left(\sum_{j \mid EMM^j_{e' \to e} > 0} EMM^j_{e' \to e} v_j \right) f_{e'm} \right) + \left(\sum_{j \mid S_{ij} < 0} S_{ij} v_j \right) f_{em} = 0 \quad m \in M_e, \ e \in E_i, \ i \in I^N \tag{3'}$$

Combined EMU e is produced by concatenating EMUs in $E_e = \{e_1, e_2, \ldots, e_{|E_e|}\}$. Let $W_{em} = \{w\} = \{(m_1, m_2, \ldots, m_{|E_e|}) | [m_n \in M_{e_n}, \forall n = 1, \cdots |E_e|] \cap [\sum_{n=1}^{|E_e|} m_n = m]\}$ be the set of every possible mass isotopomer multiplets of E_e that produce the mass isotopomer m of e. Then, f_{em} can be computed as

$$f_{em} = \sum_{w \in W_{em}} \prod_{n=1}^{|E_e|} f_{e_n m_n} \quad m \in M_e, \ e \in E^C \tag{4}$$

Note that for Eq. (3′) or (4) the heaviest mass isotopomer of each EMU is dropped due to the inherent dependency with Eq. (2).

OptMeas formulation for EMU representation

First, notice that effluxes of a metabolite always show up in the same form, the total efflux. Therefore, we introduce the new variable for the total efflux of each intermediate metabolite such that

$$V_i = -\sum_{j|S_{ij}<0} S_{ij}v_j \quad i \in I^N \tag{5}$$

Then we can rewrite (1′) and (3′) as

$$\sum_{j|S_{ij}>0} S_{ij}v_j - V_i = 0 \quad i \in I^N \tag{1}$$

$$\sum_{e' \in E}\left(\left(\sum_{j|EMM^j_{e'\to e}>0} EMM^j_{e'\to e}v_j\right)f_{e'm}\right) - V_i f_{em} = 0 \quad m \in M_e,\ e \in E_i,\ i \in I^N \tag{3}$$

We construct the incidence matrix using Eqs. (1)–(5) as in Fig. 2. Each row corresponds to an equation and each column to one of the variables that appears in the equations. We note that EMU variables are not guaranteed to be linearly independent with each other, unlike isotopomer variables. Further enhancement of the incidence matrix considering this linear dependency is discussed in Appendix B.

We next formulate the OptMeas formulation (Chang et al., 2008). We utilize the binary variable y_{rc} which is equal to one if the variable with index c is an output of the equation in row r. Correspondingly, the binary variable x_r and z_c model if row r and column c participate in any output assignments, respectively. These binary variables combine to form the incident matrix used by OptMeas. Note that we represent columns as $z_c=(z_j,z_i,z_{em})$ that correspond to v_j, V_i, f_{em}, respectively. We introduce binary variable u_e for each EMU that encodes whether EMU e is measured. Here, $u_e=1$ implies that EMU e is not measured and thus the associated EMU variables remain ones that can only be fathomed as the output of an equation. When an EMU is analyzed using MS, then all of its mass isotopomer fractions are measured and so we impose

$$z_{em} \geq u_e \quad m \in M_e,\ e \in E$$

Since V_i and f_{em} for $e \in E^C$ are not directly measurable, we enforce

$$z_i = 1 \quad i \in I^N$$
$$u_e = 1 \quad e \in E^C$$

Using this incidence matrix and these constraints, OptMeas then minimizes the sum of a weighted combination of all chosen measurements as previously described. Note that in the objective function (Eq. (7) in Chang et al. (2008)) the sum over all metabolites i is replaced by one over all EMU variables e. Accordingly, u_i and q_i are replaced by u_e and q_e, respectively, where q_e is the relative weight of EMU e.

Appendix B

Identification of linearly dependent EMU variables

Some EMU variables of a metabolite could be linearly dependent on the other EMU variables of the same metabolite. For example, there are three EMUs A_1, A_2, and A_{12} for a two-carbon metabolite A, but we can deduce the IDV of A from MDVs of A_1 and A_{12} only. Therefore, MDV of A_2 is dependent on those of A_1 and A_{12} such that $A_{2:m+0}=2A_{12:m+0}+A_{12:m+1}-A_{1:m+0}$. A linearly dependent set of all such equations can be found as follows:

(1) For each metabolite i, collect f_{em} $0 \leq m < n_e$, $e \in E_i$ into MDV_i and find the mapping MM_i (0–1 matrix) from its IDV such that $MDV_i=MM_iIDV_i$.
(2) Find the null space of $(MM_i)^t$, and denote it as NS_i (NS_i is the left-hand null space of MM_i).
(3) Find a (reduced) row-echelon form REF_i of $(NS_i)^t$ by partial pivoting (only swapping rows).

$(NS_i)^t$ has full row rank that corresponds to the linear dependency in the EMU variables, and satisfies

$$(NS_i)^t MDV_i = (NS_i)^t MM_i IDV_i = 0 \tag{6}$$

These linear homogeneous equations can replace the nonlinear balance Eqs. (3) and (4) for the EMU variables that correspond to the first nonzero column in each row of REF_i. Since the row-echelon form is not unique, this set of EMU variables is not unique.

Appendix C. Supplementary materials

Supplementary data associated with this article can be found in the online version at doi:10.1016/j.ymben.2009.10.002.

References

Antoniewicz, M.R., Kelleher, J.K., Stephanopoulos, G., 2006. Determination of confidence intervals of metabolic fluxes estimated from stable isotope measurements. Metab. Eng. 8, 324–337.
Antoniewicz, M.R., Kelleher, J.K., Stephanopoulos, G., 2007a. Elementary metabolite units (EMU): a novel framework for modeling isotopic distributions. Metab. Eng. 9, 68–86.
Antoniewicz, M.R., Kraynie, D.F., Laffend, L.A., González-Lergier, J., Kelleher, J.K., Stephanopoulos, G., 2007b. Metabolic flux analysis in a nonstationary system: fed-batch fermentation of a high yielding strain of *E. coli* producing 1,3-propanediol. Metab. Eng. 9, 277–292.
Burgard, A.P., Nikolaev, E.V., Schilling, C.H., Maranas, C.D., 2004. Flux coupling analysis of genome-scale metabolic network reconstructions. Genome Res. 14, 301–312.
Chang, Y., Suthers, P.F., Maranas, C.D., 2008. Identification of optimal measurement sets for complete flux elucidation in metabolic flux analysis experiments. Biotechnol. Bioeng. 100, 1039–1049.
Kim, H.U., Kim, T.Y., Lee, S.Y., 2008. Metabolic flux analysis and metabolic engineering of microorganisms. Mol. Biosyst. 4, 113–120.
Kleijn, R.J., van Winden, W.A., van Gulik, W.M., Heijnen, J.J., 2005. Revisiting the 13C-label distribution of the non-oxidative branch of the pentose phosphate pathway based upon kinetic and genetic evidence. FEBS J. 272, 4970–4982.
Reed, J.L., Vo, T.D., Schilling, C.H., Palsson, B.O., 2003. An expanded genome-scale model of *Escherichia coli* K-12 (iJR904 GSM/GPR). Genome Biol. 4, R54.
Schmidt, K., Carlsen, M., Nielsen, J., Villadsen, J., 1997. Modeling isotopomer distributions in biochemical networks using isotopomer mapping matrices. Biotechnol. Bioeng. 55, 831–840.
Suthers, P.F., Burgard, A.P., Dasika, M.S., Nowroozi, F., Van Dien, S., Keasling, J.D., Maranas, C.D., 2007. Metabolic flux elucidation for large-scale models using (13)C labeled isotopes. Metab. Eng. 9, 387–405.
Wiechert, W., Mollney, M., Isermann, N., Wurzel, M., de Graaf, A.A., 1999. Bidirectional reaction steps in metabolic networks: III. Explicit solution and analysis of isotopomer labeling systems. Biotechnol. Bioeng. 66, 69–85.
Young, J.D., Walther, J.L., Antoniewicz, M.R., Yoo, H., Stephanopoulos, G., 2007. An elementary metabolite unit (EMU) based method of isotopically nonstationary flux analysis. Biotechnol. Bioeng. 99, 686–699.
Zupke, C., Stephanopoulos, G., 1994. Modeling of isotope distributions and intracellular fluxes in metabolic networks using atom mapping matrices. Biotechnol. Prog. 10, 489–498.